

Kinetic and Product Distribution Modeling of Fischer-Tropsch Synthesis in a Fluidized Bed Reactor

Mojtaba Nabipoor Hassankiadeh, Ali Khajehfard, and Morteza Golmohammadi

Abstract—A mathematical model for the Fischer-Tropsch synthesis in a fluidized bed reactor was developed. A comprehensive kinetic model was applied for modeling of a fluidized bed reactor so that the CO conversion was correlated with good accuracy over the range of the reactor conditions of 523-563K, 0.95-2.55MPa and H₂/CO ratio 0.65-1.51. Using the comprehensive kinetic model, the results of CO conversion in a fluidized bed reactor showed a very good agreement with the experiment. The results of modeling showed that the Average Absolute Deviation percentage (AAD %) of 8.98% for CO conversion. In addition, a proper product distribution model for FT process using the appropriate kinetic model has been developed. The results revealed only 8.09% deviation from the olefin experimental data and 10.27% deviation from the paraffin experimental data that is acceptable in comparison with previous literatures.

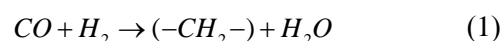
Index Terms—Fischer-tropsch synthesis, fluidized-bed reactor, kinetic modelling, product distribution

I. INTRODUCTION

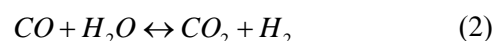
Welcome in the Fischer-Tropsch (FT) process, synthesis gas, a mixture of predominantly CO and H₂, obtained from coal, peat biomass or natural gas which converted to a multicomponent mixture of hydrocarbons [1]. Currently, a promising topic in the energy industry is the conversion of remote natural gas to environmentally clean fuels, especially chemicals and waxes. Fuels produced with the FT process are of high quality due to a very low aromaticity and absence of sulfur. These fuels can be used as blending stocks for transportation fuels derived from crude oil. Other valuable products besides fuels can be tailor-made with the FT in combination with upgrade processes: for example, ethane, propane, α -olefins, ketones, solvents, alcohols, and waxes [2].

The FT process is catalyzed by both iron and cobalt at pressures from 10 to 60 bar and temperatures from 200 to 300 °C [3]. The FT synthesis is a surface polymerization reaction. The reactions, CO and H₂, absorb and dissociate at the surface of the catalyst and react to form chain initiator (CH₃), methylene (CH₂) monomer and water. The hydrocarbons are formed by CH₂ insertion into metal-alkyl bonds and subsequent dehydrogenation or hydrogenation to an α -olefin or paraffin, respectively. Iron catalysts can also use synthesis gas with a H₂/CO ratio below 2, because excess

of CO is converted with water to carbon dioxide and hydrogen in the water gas shift (WGS) reaction [3, 4]. The most important aspects for FT reactor development are the high reaction heats and the large number of products (gas, liquid and waxy hydrocarbons) [2]. The main reaction of the Fischer-Tropsch synthesis for synthesis gas (Syngas) conversion is presented as [3]:



The WGS occurs over iron catalyst according to the equation below [3]:



Many researchers have been working on catalyst development [1, 2], reactor design [3]-[6], and on the commercial applications of the Fischer-Tropsch synthesis [7, 8], but few investigations have been done in order to optimize production of specific products.

The product distributions tend to obey the Anderson-Shultz-Flory (ASF) chain-length statistics, but this is not always true, and many researchers have reported deviations from the ASF theory [9-11]. Theories for ASF deviations are based in the superposition of two ASF distributions and rely in the dual site theory [11], secondary chain growth of reabsorbed alkenes theory, and the dual mechanism of chain growth theory [12, 13]. Iron catalysts are more likely to obey dual mechanism of chain growth theory.

II. MASS BALANCE IN TWO PHASE FLOW

Gas Phase is considered as bubbles with a constant volume. The gas bubbles move up through the reactor and due to differences in concentration of reactants in the gas phase and liquid Reactivity material is transferred of the gas phase to the liquid, Then transferred from liquid to solid surfaces And in the solid phase reaction products are produced. So the mass balance equation for the gas phase is written as below:

$$\varepsilon^g V_z^g \frac{dC_i^g}{dz} + (K_L a_L)_i (C_i^{g'} - C_i^L) = 0 \quad (3)$$

That ε^g is gas phase holdup, V_z the average velocity of each phase in the Z direction, K_L Gas to liquid mass transfer coefficient, a_L Special surface of gas bubbles and $C_i^{g'}$ Equilibrium concentration of component i in the gas-liquid which was obtained from the relationship that we have in the ideal solution.

Manuscript received September 10, 2012; revised November 28, 2012.

Mojtaba Nabipoor Hassankiadeh and Ali Khajehfard are with the Process Engineer of South Pars Gas Complex (SPGC), Phases 9&10, Assaluyeh, Iran (e-mail: mojtabanp@yahoo.com).

Morteza Golmohammadi is with the School of Chemical Engineering, College of Engineering, University of Tehran.

$$C_i^{g'} = \frac{C_i^g \times RT}{He_i} \quad (4)$$

where He_i is Henry constant of component i , putting the equation (4) in equation (3), the gas phase mass balance would be:

$$\varepsilon^g V_Z^g \frac{dC_i^g}{dZ} + (K_L a_L)_i \left(\frac{RTC_i^g}{He_i} - C_i^L \right) = 0 \quad (5)$$

Considering that the defaults for the gas phase had the same assumptions for the liquid phase is established, liquid phase in two ways which companies in mass balance. Article reactivity due to the concentration of the liquid into the gas phase, and the reaction product is produced. Article reactivity due to the concentration of the liquid into the gas phase, and the reaction product is produced. So for any component of the following mass balance equations are written:

$$\varepsilon^L V_Z^L \frac{dC_i^L}{dZ} - (K_L a_L)_i \left(\frac{RTC_i^g}{He_i} - C_i^L \right) + \rho_s \varepsilon_s \varepsilon_L \left[\sum v_j R_j \right] = 0 \quad (6)$$

In the Eqs. (5) and (6) instead R_j , it can be placed R_{WGS} and R_{FTS} . The finite differences are used to numerically solve the model differential equations, whereas the simplex method is used to estimate the adaptive rate parameters.

III. KINETIC MODEL

Different models have been used for kinetic modeling of Fischer-Tropsch synthesis in the presence of iron catalyst. In this study a comprehensive kinetic model which has lowest error than the other models, has been used [14]:

$$r_{FT} = \frac{k_{FT} P_{CO}^{\frac{1}{2}} P_{H_2}^{\frac{1}{2}}}{\left(1 + K_1 P_{H_2}^{\frac{1}{2}} + K_2 P_{CO}^{\frac{1}{2}} + K_3 P_{CO} \right)^2} \quad (7)$$

Water gas shift reaction (WGS) kinetic model used for modeling is as follows:

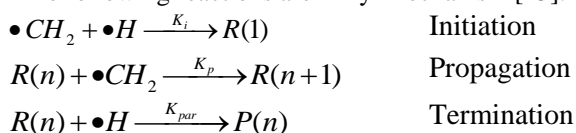
$$r_{WGS} = \frac{K_{WGS} \left(P_{CO} P_{H_2O} / P_{H_2} - P_{CO_2} P_{H_2}^{\frac{1}{2}} / K_p \right)}{\left(1 + K_4 P_{CO} + K_5 P_{H_2O} \right)^2} \quad (8)$$

IV. PRODUCT DISTRIBUTION IN FLUIDIZED BED REACTORS

There are two main mechanisms for product distribution in Fischer-Tropsch synthesis. They are Alkyl and Alkenyl mechanism [15]. In response to the Fischer-Tropsch series of reactions such as polymeric reactions, the initiation, propagation, and termination reactions are used.

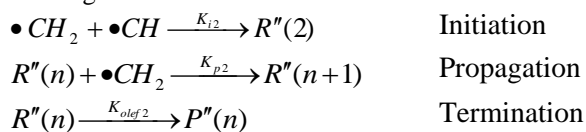
A. Alkyl Mechanism

The following reactions are Alkyl mechanism [15]:



B. Alkenyl Mechanism

The Alkenyl mechanism can be represented by the following reaction:



Considering Alkyl and Alkenyl mechanism the mass balance equations is presented as following:

$$R(1) = \frac{k_i \cdot P_{H_2}}{k_p} \quad (10)$$

$$R''(2) = \frac{k_{i2} \cdot R_{FTS}}{k_{p2}} \quad (11)$$

$$R(n) = \frac{k_p \cdot R_{FTS}}{k_p \cdot R_{FTS} + k_{par} \cdot P_{H_2} + k_{olef}} \cdot R(n-1) \quad (12)$$

$$R''(n) = \frac{k_{p2} \cdot R_{FTS}}{k_{p2} \cdot R_{FTS} + k_{olef2}} \cdot R''(n-1) \quad (13)$$

$$\frac{dP(1)}{dt} = k_{met} \cdot P_{H_2} \cdot R(1) \quad (14)$$

$$\frac{dP(2)}{dt} = k_{et} \cdot P_{H_2} \cdot R(2) \quad (15)$$

$$\frac{dP''(2)}{dt} = k_{O_2} \cdot R_{FTS}^2 \quad (16)$$

$$\frac{dP(n)}{dt} = k_{par} \cdot P_{H_2} \cdot R(n) \quad (17)$$

$$\frac{dP''(n)}{dt} = k_{olef} \cdot R(n) + k_{olef2} \cdot R''(n) \quad (18)$$

Equations can be solved simultaneously with the concentration of paraffins and olefins, according to a specified number of carbon gains.

V. RESULTS AND DISCUSSION

In this work at first, the finite difference is used to numerically solve the model differential equation (5 and 6), whereas the simplex method is used to estimate the adaptive rate parameters. During the optimization procedure our objective function is defined in a way to minimize the average absolute deviation percentage (AAD %) which is expressed as below:

$$AAD\% = \frac{1}{n} \sum_{i=1}^n \left| \frac{X_{CO}^{cal} - X_{CO}^{exp}}{X_{CO}^{exp}} \right| \times 100 \quad (19)$$

In order to evaluate the new developed kinetic model, the

experimental data given by Chang et al. has been employed [16]. For modeling of the fluidized bed reactor, Langmuir-Hinshelwood isotherm has been used for both the FTS and WGS and results of this study showed that AAD% is about 8.98 for the CO conversion. Fig. 1 shows the calculated values of the CO conversion versus the experimental data using LH model.

After calculating the optimized rate constants, the computation of the product distribution of reactants was developed. By solving Eqs. (10-18) simultaneously and using the 4th order Runge-Kutta, the product distribution in the fluidized bed reactor can be modeled. The product distribution parameters for Alkyl and Alkenyl mechanism for the polymerization of carbon monoxide are given in Table I.

Fig. 2 shows the results of the parameter estimation obtained for the model proposed by Raje&Davis kinetic model. Fig. 3 depicts the product distribution for paraffins and olefins at $T=523\text{K}$, $H_2/CO=0.67$ and $P=1.45\text{MPa}$. Considering the optimized product distribution which obtained in this study, paraffin deviation from experimental data is 10.27 and for olefins is 8.09 that is more acceptable result comparing to the previous results reported in literatures [1,15].

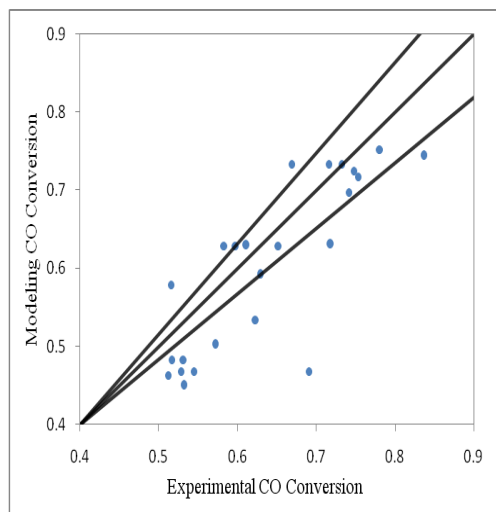


Fig. 1. The calculated conversion of CO against the experimental conversion using LH model

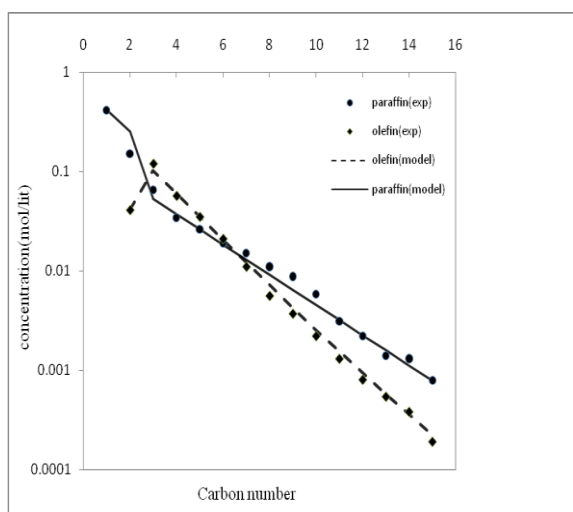


Fig. 2. Carbon number distributions of paraffins and olefins for $T=523\text{K}$, $H_2/CO=0.67$ and $P=1.45\text{MPa}$ with Raje&Davis kinetic model. Symbols refer to experimental data and lines to model simulations result.

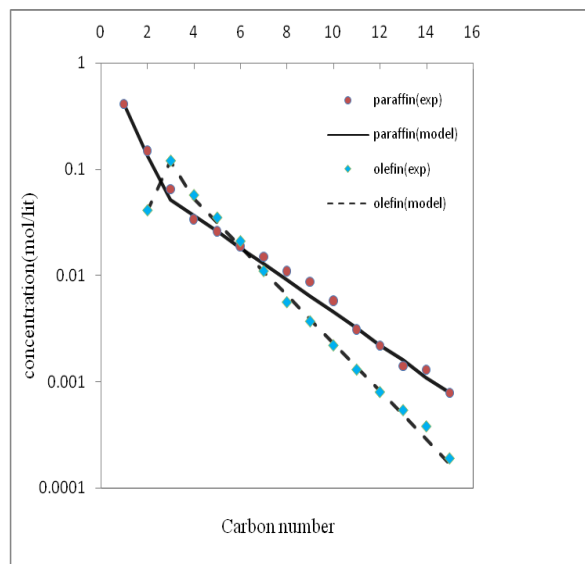


Fig. 3. Carbon number distributions of paraffins and olefins for $T=523\text{K}$, $H_2/CO=0.67$ and $P=1.45\text{MPa}$. Symbols refer to experimental data and lines to model simulations result.

TABLE I: KINETIC PARAMETERS FOR ALKYL AND ALKENYL PRODUCT DISTRIBUTION MODEL

$k_i(\text{Mpa}^{-1})$	$8.03 \cdot 10^{-2}$
$k_{i2}(\text{mol/h})$	$8.73 \cdot 10^{-2}$
$k_p(\text{h/mol})$	$3.07 \cdot 10^2$
$k_{p2}(\text{h/mol})$	$2.03 \cdot 10^{-1}$
$k_{par}(\text{Mpa}^{-1}\text{h}^{-1})$	1.87
$k_{olef}(\text{h}^{-1})$	$5.22 \cdot 10^{-1}$
$k_{olef2}(\text{h}^{-1})$	1.07
$k_{met}(\text{Mpa}^{-1}\text{h}^{-1})$	7.28
$k_{et}(\text{Mpa}^{-1}\text{h}^{-1})$	3.37
$K_{O_2}(\text{h/mol})$	$1.23 \cdot 10^{-1}$

VI. CONCLUSION

In this work a comprehensive kinetic model was developed in fluidized bed reactor. Using Langmuir-Hinshelwood kinetic model, the results of CO conversion in a fluidized bed reactor showed a very good agreement with the experiment. The results of modeling showed that the AAD of 8.98% calculated for CO conversion. The product distribution of Fischer Tropsch synthesis also was studied using the dual mechanism theory. Dual mechanism theory predicts the products of FTS using the alkyl and Alkenyl mechanism. Whereas, the Raje&Davis reaction rate is simple, we used another reaction rate equations based on the Langmuir-Hinshelwood isotherm. The results revealed only 8.09% deviation from the olefin experimental data and 10.27% deviation from the paraffin experimental data that is acceptable in comparison with previous literatures.

ACKNOWLEDGMENT

Financial assistance from the National Iranian Gas Company and South Pars Gas Complex (SPGC) is gratefully acknowledged.

REFERENCES

- [1] A. P. Raje and B. H. Davis, "Fischer-Tropsch synthesis over iron-based catalysts a slurry reaction rate, selectivities and implications for improving hydrocarbon," *Catal. Tod.*, vol. 36, pp. 335-345, 1997.

- [2] F. V. Steen and H. Schulz, "Polymerization kinetics of the Fischer-Tropsch CO hydrogenation using iron and cobalt based catalysts," *Appl. Catal. A.*, vol. 186, pp. 309-320, 1999.
- [3] C. Maretto and R. Krishna, "Modeling of bubble column slurry reactor for Fischer-Tropsch synthesis," *Catal. Tod.*, vol. 52, pp. 279-289, 1999.
- [4] R. Krishna and S. T. Sie, "Design and scale up of the Fischer-Tropsch bubble column slurry reactor," *Fuel Proc. Tech.*, vol. 64, pp. 73-105, 2000.
- [5] R. Krishna, J. M. V. Baten, and M. I. Urseanu, "J. Ellenberger. Design and scale up of a bubble column slurry reactor for Fischer-Tropsch synthesis," *Chem. Eng. Sci.*, vol. 56, pp. 537-545, 2001.
- [6] Y. N. Wang, Y. Y. Xu, Y. W. Li, Y. L. Zhao, and B. J. Zhang, "Heterogeneous modeling for fixed bed Fischer-Tropsch synthesis: reactor model and its applications," *Chem. Eng. Sci.*, vol. 58, pp. 867-875, 2003.
- [7] C. K. Mossgas, "Gas to liquid diesel fuels—an environmentally friendly option," *Catal. Tod.*, vol. 71, pp. 437-445, 2002.
- [8] D. J. Wilhem, D. R. Simbeck, A. D. Karp, and R. L. Dickenson, "Syngas production for gas-to-liquids applications: technologies, issues and outlook," *Fuel Proc. Tech.*, vol. 71, pp. 139-148, 2001.
- [9] G. A. Huff and C. N. Satterfield, "Evidence for two chain growth probabilities on iron catalysts in the Fischer-Tropsch synthesis," *J. Catal.*, vol. 85, pp. 370-379, 1984.
- [10] E. Iglesia, S. C. Reyes, and R. J. Madon, "Transport-enhanced α -Olefin readsorption Pathway in Ru-Catalyzed Hydrocarbon Synthesis," *J. Catal.*, vol. 129, pp. 238-247, 1991.
- [11] R. J. Madon and W. F. Taylor, "Fischer-Tropsch synthesis on a precipitated iron catalyst," *J. Catal.*, vol. 69, pp. 32-43, 1981.
- [12] J. Patzlaff, Y. Liu, C. Graffmann, and J. Gaube, "Studies on product distribution of iron and cobalt catalyzed Fischer-Tropsch synthesis," *Appl. Catal. A.*, vol. 86, pp. 109-117, 1999.
- [13] J. Patzlaff, Y. Liu, C. Graffmann, and J. Gaube, "Interpretation and kinetic modeling of product distributions of cobalt catalyzed Fischer-Tropsch synthesis," *Catal. Tod.*, vol. 71, pp. 381-394, 2002.
- [14] A. Haghtalab, M. Nabipoor, and S. Farzad, "Kinetic modeling of Fischer-Tropsch synthesis in a slurry bubble column reactor using Langmuir-Freundlich isotherm," *Fuel Proc. Tech.*, 2011.
- [15] F. A. N. Fernandes, "Polymerization kinetics of fischer-tropsch reaction on iron based catalysts and product grade optimization," *Chem. Eng. Technol.*, vol. 28, pp. 930-938, 2005.
- [16] J. Chang, L. Bai, B.-T. Teng, R. L. Zhang, J. Yang, Y. Y. Xu, H. W. Xiang, and Y. W. Li, "Kinetic modeling of Fischer-Tropsch synthesis over Fe.Cu.K.SiO₂ catalyst in slurry phase reactor," *Chem. Eng. Sci.*, vol. 62, pp. 4983-4991, 2007.